POLITECNICO DI TORINO
Repository ISTITUZIONALE

Thermo-mechanical properties enhancement of bio-polyamides (PA10.10 and PA6.10) by using rice husk ash and nanoclay

Original
Thermo-mechanical properties enhancement of bio-polyamides (PA10.10 and PA6.10) by using rice husk ash and nanoclay / Battegazzore, D., Salvetti, O., Frache, A., Peduto, N., De Sio, A., Marino, F.. - In: COMPOSITES. PART A: APPLIED SCIENCE AND MANUFACTURING. - ISSN 1359-835X. - STAMPA. - 81:(2016), pp. 193-201. [10.1016/j.compositesa.2015.11.022]

Availability:
This version is available at: 11583/2624991 since: 2022-06-17T17:18:27Z

Publisher:
ELSEVIER SCI LTD, THE BOULEVARD, LANGFORD LANE, KIDLINGTON, OXFORD, ENGLAND

Published
DOI:10.1016/j.compositesa.2015.11.022

Terms of use:

This article is made available under terms and conditions as specified in the corresponding bibliographic description in the repository

Publisher copyright
Elsevier postprint/Author's Accepted Manuscript

© 2016. This manuscript version is made available under the CC-BY-NC-ND 4.0 license
http://creativecommons.org/licenses/by-nc-nd/4.0/.The final authenticated version is available online at:
http://dx.doi.org/10.1016/j.compositesa.2015.11.022

(Article begins on next page)

19 November 2026

Thermo-mechanical properties enhancement of Bio–polyamides (PA10.10 and PA6.10) by using rice husk ash and nanoclay.

Daniele Battegazzore[a*], Oreste Salvetti[a], Alberto Frache[a*], Nicolangelo Peduto[b], Anna De Sio[b], Francesco Marino[a]

[a]Dipartimento di Scienza Applicata e Tecnologia, Politecnico di Torino, sede di Alessandria, Viale Teresa Michel 5, 15121 Alessandria, Italy

[b]Radici Chimica SpA, Via Fauser 6 Novara

[*]Corresponding author: Tel/Fax: +390131229343/+390131229399; e-mail address: daniele.battegazzore@polito.it

Abstract

Composites consisting of fully (PA10.10) and partially (PA6.10) bio-based polyamides and 10–20 wt.% rice husk ash (RHA) was prepared by melt compounding. The mechanical analysis data showed that RHA induced significant improvement in Young's modulus, a slight reduction in the tensile strength and a large decrease in the deformation at break. Pukanszky's model was used to evaluate the filler-matrix interactions. The two PAs exhibited similar filler-matrix load transfer with RHA and better performance than polylactic acid (PLA). The addition of modified clay (Cloisite 30B) to the systems with 10 wt.% of RHA gave the best mechanical properties and filler-matrix interactions, notwithstanding the matrix used. Finally, DMT analyses demonstrated that the addition of RHA caused an increase in the heat deflection temperature (HDT) compared to the neat PA matrices. Furthermore, the simultaneous presence of RHA and clay provided the best results.

Keywords:

A. Biocomposite; A. Polymer-matrix composites (PMCs); B. Adhesion; B. Thermomechanical.

1. Introduction

Because of the increasing awareness about environmental impact, new legislations/regulations and recycling of materials, considerable work has been performed for replacing plastics derived from petrol chemistry (fossil-based polymers) with those derived from bio-sources. Among them, biodegradable polymers such as PLA (polylactic acid), PHAs (polyhydroxyalkanoates), starch, cellulose, and non-biodegradable polymers such as PE (polyethylene), PET (polyethylene terephthalate), PAs (polyamides), can be considered the most representative examples.

From an overall consideration, the field of bio-based polymers is continuously growing, as is clear from the forecast data published by European Bioplastics [1]. Among the bio-based polymers, some aliphatic polyamides were recently revalued by industries for new long-term applications. Generally, polyamides (i.e. PA 6 and PA 6.6) are well known as materials with relatively high strength, high ductility, excellent resistance to short term heat exposure, and good resistance to chemicals. Conversely, completely bio-based polyamides (PA 10.10 and PA 11) do not exhibit comparable performances. Hence, there is a need to have an in-depth understanding of these compounds and to study them for further improvement. In particular, one of their main drawbacks is their poor thermo-mechanical properties. In general, investigators in this field usually

adopted the methods of polymer blending and addition of inorganics to improve such properties [2-4].

Conventional fillers used with polymers are silica, talc, kaolin, mica, calcium carbonate, glass fiber, and carbon fiber. Among nonconventional fillers, natural fibers have gained commercial importance and there are numerous studies indicating that the performance of natural by-products or industrial waste is comparable to that of commercial fillers such as silica or talc, notwithstanding the environmental aspect [5-6]. Recently, two studies on the use of cellulose [7] and silica [8] obtained from rice husk with PLA have been published. In these papers it is found that the incorporation of cellulose or silica results in significant improvement of Young's modulus as well as a slight reduction in the oxygen permeability of PLA.

In another two very recent works Feldmann et al. evaluated the influence of compounding parameters and temperature settings on the mechanical properties of short man-made cellulose fiber in PA 10.10 [9] and compared the mechanical properties of the same filler in PA 6.10, 10.10 and PA 6 [10]. In this last paper they also reported relevant enhancement of HDT for the two bio-polyamides.

These important results have lead the possibility of obtaining good thermo-mechanical results in the case of bio-polyamides and natural by-products. In particular, this paper is focused on the use of the ash that is obtained from the combustion of the rice husk. Indeed, rice husk (RH) is an agricultural by-product that is inexpensive and available abundantly. The yearly global paddy production has been estimated to be 749 million tons for 2015, which implies about 150 million tons of RH production [11]. There are several uses of RH [12-13] but it is still often considered a waste product of rice milling, and thus, often burned in open air or dumped in wastelands. Furthermore, it is well

known that RH can be also used as a renewable fuel in cogenerating plants, considering its high calorific value (4012 Kcal/kg) [14]. During its combustion, about 20–25 wt.% of rice husk ash (RHA), containing approximately 55–97 % of silica (depending upon the combustion conditions), with traces of carbon impurity and other metal oxides, is produced [15]. This new by-product has been widely used as a filler in polymers [16–21] but never in PA10.10.

On the other hand, in the last twenty years, compounding with clay at the nanoscale level has attracted great interest among polymer scientists. Furthermore, the incorporation of fillers, especially at the nanoscale level, has proved to be an effective way of enhancing the mechanical properties of polyamides [22]. Indeed, nanocomposites frequently exhibit excellent physical and mechanical properties with less than 5 wt.% addition, such as improved strength, enhanced modulus, and increased thermal stability compared to those of neat polymers. These findings were attributed to the nanoscale dispersion of clay in the polymer matrix, high aspect ratio of the lamellae and interfacial interaction between clays and polymers. Some studies have been performed on the use of renewable PA with clays [23] that exhibit an interesting enhancement in the thermo-mechanical properties.

The aim of this work has been to produce PA10.10-based bio-composites using a cheap and commercially available by-product, RHA. Subsequently, a detailed study of the morphological observation by SEM was used to correlate the microstructures to the mechanical properties. In addition, mechanical performances, with particular attention to heat deflection temperature (HDT), was compared with that of a partially renewable polyamide (PA6.10) and with the most commonly used bio-degradable polymer (PLA). The second goal of the study was to investigate if the combined use of micro and nano

fillers gave some further improvement. To this aim, RHA and clay composites were produced and compared with the previous ones.

2. Material and methods

2.1 Materials

2.1.1 Polyamides production

Two kinds of Polyamide: PA6.10 and PA10.10 were produced by Radici Chimica SpA. The two PAs have only the "10" structural unit derived from renewable resources (castor oil). An overview of the process to obtain the polymers are hereafter presented. The Sebacic acid used in the production of the bio-PAs can be obtained either starting directly from castor oil or starting from the fatty acids obtained from castor oil by a saponification reaction [24-25]. The last procedure may lead to a higher reaction yield and it implies the use of the fatty acids mixed with NaOH and eventually a catalyst (cadmium) under pressure in a stainless steel stirred reactor (autoclave). The autoclave is preliminarily filled with H_2 and maintained at a pressure of about 55 bar for about 20 minutes to eliminate oxygen in the reaction mix. Pressure is then released and heating is carried out in order to achieve the reaction temperature of 300-320°C that is maintained for a certain period of time (usually about 2 hours). When the reaction is completed, the autoclave is cooled down and the reaction mix dissolved or diluted in water. The azeotrope water – 2 octanol, which is the main by-product, is then driven off with steam after the acidification of the solution with sulfuric acid to a pH of about 6. While fatty acids are precipitated, sodium sabacate remains dissolved in the solution and it is readily filterable. The filtrated solution is further acidified till pH 2 with sulfuric acid. In this conditions sodium sebacate became sabacic acid, not soluble in water. Thus,

sebacic acid could be recovered by filtration, washed with water and dried at 90°C. The melting point of the obtained sebacic acid is between 130–132°C.

The Polyamide 6.10 used in the present study is obtained by reacting aqueous salt solution at a temperature below 300 °C, e.g. 285–290°C, and at a pressure of approximately 18 bar for a suitable time, usually around 3 hours. In a first step, salt preparation, the sebacic acid is dissolved in water at a temperature of 50°C followed by the addition of a stoichiometric quantity of hexamethylene diamine (HMDA). The addition of HMDA is carried out considering the possible loss of a part of diamine during the process. The pH of the solution is adjusted according to the desired MW of the resin. Usually the pH of the salt is measured and adjusted to a value between 7.3 and 8.6, adding either HMDA or sebacic acid. The mixture is agitated and heated at about 60°C to maintain the salt in solution. The concentration to get a clear solution is about 40 wt.-% of salt.

In the second step, the polymerization one, the salt is transferred in a stirred autoclave, heated up to 225°C, with a pressure of 17.5 bar. This pressure level is maintained constant by slowly bled off the water vapor and the temperature achieves 260°C. This pre-polymerization phase carried out over about 90 minutes. Subsequently, the pressure is slowly reduced to atmospheric one in about 90 minutes and the temperature is increased to 285°C. The final finish phase is carried out for about 60 minutes with the temperature raising till 290°C. The polymer is then extruded through a die, quenched in cold water, and cut into small pellets.

The preparation of PA 10.10 follows the same procedure already described for PA 6.10. The starting monomers are 1,10 decanediamine and sebacic acid, both derived from castor oil and thus 100% bio-based. Compared to PA 6.10 process, the first step has a

different concentration of monomers owing to a low solubility of the decanediamine in water.

The resulting materials have renewable carbon content, determined by radiocarbon analysis, ranging from 98% to 60% for PA10.10 and PA6.10, respectively.

2.1.2 PLA

Poly(lactic acid) (PLA) (4042D grade), was purchased from NatureWorks LLC and used for preparing comparison samples.

2.1.3 Fillers

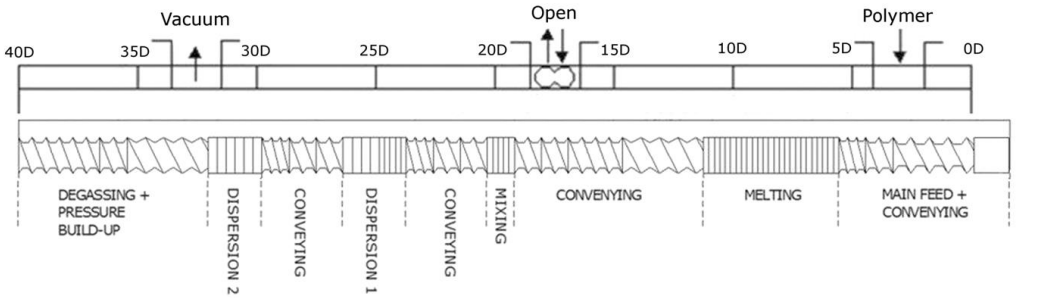
The fillers, rise husk ash (RHA) (MICRO SILICA MS 325) (density = 2.18–2.3 g/cm^3, specific surface = 15–30 m^2/g, particle dimension = 325 mesh), and a natural montmorillonite modified with methyl hydrogenated tallow bis-2-hydroxyethyl quaternary ammonium, (Cloisite®30B-Cl30B), were purchased from SB Sílica Brasil Ltda. and Southern Clay Products Inc., respectively.

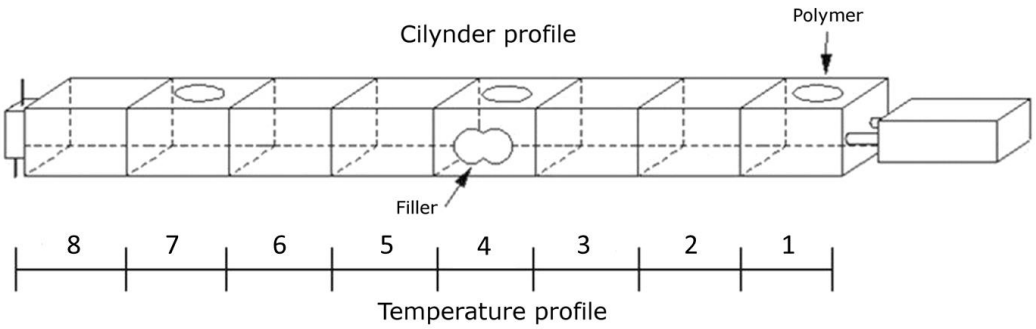
2.2 Composite preparation

All PAs and PLA were dried at 80°C for 8 h in an industrial dryer from Piovan before extrusion, reaching <200 ppm of water content, assessed by Karl-Fisher titration. Analogously, both RHA and Cl30B were dried before the extrusion in a vacuum convection oven at 120°C for 5 h, as well.

Table 1. Codes and compositions of melt-blended PA- and PLA-based samples.

Sample	PA [wt.%]	PLA [wt.%]	RHA [wt.%]	Cl30B [wt.%]	Content of renewable sources [%]
PA6.10_10S	90.0	-	10.0	-	64.0
PA6.10_20S	80.0	-	20.0	-	68.0
PA6.10_10S5C	85.0	-	10.0	5.0	64.5
PA10.10_10S	90.0	-	10.0	-	98.2
PA10.10_20S	80.0	-	20.0	-	98.4
PA10.10_10S5C	85.0	-	10.0	5.0	96.8
PLA_20S	-	80.0	20.0	-	100.0
PLA_10S5C	-	85.0	10.0	5.0	98.50





[°C]	[°C]	[°C]	°C]	[°C]	[°C]	[°C]	[°C]	Sample
230	230	240	240	240	250	250	250	PA6.10
210	210	220	220	220	230	230	230	PA10.10
185	185	190	190	195	195	200	200	PLA

Figure 1. Twin screw profile and set temperatures of the eight thermo-stated barrel blocks.

PA- and PLA-based composites with different filler content (**Table 1**) were melt blended using a co-rotating twin screw extruder LEISTRITZ ZSE 27/40 D (diameters). The screw speed was fixed at 180 rpm. The heating temperature was set into the eight thermo-stated barrel blocks as reported in **Figure 1**. Two gravimetric feeders were used: namely, the main hopper for the polymer was placed at the beginning of the screw and the second one (side feeder) for the filler in the middle of the barrel. Close to the screw end, a degassing hole in the barrel connected to a vacuum pump was present (**Figure 1**). The total extrusion flow rate was fixed at 8 kg/h. The used screw profile is reported in **Figure 1** and was optimized in a previous work [8]. Hereafter, the samples will be coded on the basis of the type, nominal compositions, and filler origin as reported in **Table 1**.

Pellets obtained by extrusion were dried at 80°C for 8 h in a vacuum convection oven before the preparation of suitable specimens for stress-strain and dynamic-mechanical thermal analyses (DMTA)

The samples for stress-strain analyses (5B type specimens according to the standard ISO527) and DMTA ($6.4 \times 3 \times 60$ mm^3) were prepared using the injection molding machine Babyplast 6/10P.

2.3 Characterization techniques

The morphology of the composites was studied using a ZEISS Supra 40 FE-SEM Scanning Electron Microscope. The samples were obtained by fracturing specimens in

liquid nitrogen. These pieces were pinned up with conductive adhesive tapes and metallized using chrome.

Tensile tests were performed at room temperature (23±1°C) using a Zwick Roell Z100 machine, following the ISO 527 standard, under a loading cell of 5 kN and a rate of 1 mm/min. Using this first step, the tensile modulus was calculated; subsequently, the rate was increased up to 5 mm/min until the specimen broke. The samples for stress-strain analyses was 5B type specimen according to the standard ISO527.

Ten specimens were used for each formulation and the average values and corresponding standard deviations were calculated. These tests provided the Young's modulus values (E), elongation at break (ε), and maximum and yield tensile strength (σ_{max} and σ_y) of the bio-composites.

Dynamic-mechanical thermal experiments (DMTA) were performed using a DMA Q800 (TA Instruments) using a dual cantilever clamp. The experimental conditions were: temperature range from 30 to 180ºC, heating rate of 3ºC/min, 1 Hz frequency, and 0.05% of oscillation amplitude.

Prior to mechanical tests, all specimens were conditioned at 23±1°C and 50% relative humidity in a climatic chamber for minimum 48 h.

2.4 Experimental data analysis

Morphological analysis

In order to describe the morphology of the loaded samples statistically, two different parameters were investigated: distribution and dispersion. Both were evaluated using 250x magnification images.

The distribution parameters were calculated to provide a quantitative idea of the variation of the particle numbers in equal surrounding areas. For this reason, the

pictures were split into nine identical rectangles. For each of the nine areas the number of particles is estimated and then the mean value is calculated. The determined mean value was subtracted from the particle number of each of the nine areas. In this way, these nine numbers gave the particle number variation of each area with respect to the average value. To be able to compare different filler loadings, the observed differences were normalized as a percentage of the total number of particles, and in this case, the average was also calculated.

The second parameter taken into account for the morphological analysis was the dispersion. Analogously to what has already been done and using the same pictures, the particles were numbered, but, this time, in relation to their dimensions. In order to evaluate the distribution of particle dimensions, four different ranges were selected (up to 5 µm, from 5 to 10 µm, from 10 to 50 µm, and over 50 µm). Again, the data collected were normalized and reported as percentage versus the dimension range for every composition. In doing so, it is possible to compare the distribution of particle sizes in the different polymers and evaluate the effect of the extrusion process on the particles with different matrices. The limit of this technique is the lower limit of investigation, which is around 2–3 µm.

Mechanical data analysis

Stress-strain and DMT analyses were employed to mechanically characterize the samples in order to:

i) assess the effect of filler content and type on Young's modulus, elongation at break, and maximum tensile strength at room temperature.

ii) evaluate the filler-matrix interactions with Pukanszky's model.

The effect of polymer-filler interactions can be quantitatively described using Pukanszky's model for particle-based composites, as described in **Equations (4)** and **(5)** **[**26].

Specifically, **Equation (5),** derived from **Equation (4),** allows us to investigate a linear relationship between the natural logarithm of reduced yield stress σ_{red} (defined as follows) and the filler content [27-28].

$$\sigma_c = \sigma_m \frac{1-\phi_f}{1+2.5\phi_f} \exp\left(B\phi_f\right)$$

Equation (4)

$$log(\sigma_{red}) = log\frac{\sigma_c\left(1+2.5\phi_f\right)}{\sigma_m\left(1-\phi_f\right)} = B\phi_f$$

Equation (5)

where σ_c and σ_m are the yield stresses (σ_y) of the composite and matrix, respectively; B is a term corresponding to the load carrying capability of the filler and depends on filler-matrix interactions; and ϕ_f is the filler volumetric fraction within the polymer matrix. For the application of this model, it is necessary to know the volumetric fractions, and thus the RHA and Cl30B density within the composites. In order to determine the RHA and Cl30B densities, Archimedes' law was used, performing weight measurements in air and water. Matrix densities used were 1.05 for the two PA and 1.25 g/cm^3 for PLA, as reported in the manufacturer data sheets. A density value of 1.7 and 1.63 g/cm^3 for the RHA and RHA-Cl30B (ratio 2:1) has been found. Subsequently, these values have been used for calculating the volumetric fractions (ϕ) required by the model (0.064, 0.134, and 0.102 for 10S, 20S, and 10S5C, respectively, and 1.154 and 1.180 for PLA20S and PLA10S5C, respectively).

In our manuscript, such a model was used for assessing PA-filler interactions and for establishing if some differences occur upon changing the bio-matrix.

iii) assess the effect of filler content and type on storage modulus over the 30–180°C range.

iv) evaluate the heat deflection temperature (HDT) of composites.

The HDT softening test described by ASTM D-648 represents the standardized test to characterize elevated temperature performance in plastic materials. The HDT test is essentially designed to evaluate the temperature at which a specific deformation occurs in a 3-point bending mode under a specific load (0.455 MPa or 1.82 MPa). These single points are often industrially used in the material selection process as the maximum continuous use temperatures. The HDT defines a temperature at which a sample exhibits a specific deformation, and the test essentially measures the temperature at which a material achieves a certain modulus. Takemori [29] has calculated the modulus values that correspond to specific loads: 800 and 200 MPa for the applied load of 1.82 and 0.455 MPa, respectively. In this study, the two HDTs have been calculated as the temperature at which the modulus crosses previously defined values.

ASTM D-648 defines two stress levels for measuring the heat deflection temperature: method A corresponds to the high-load and method B for the low-load conditions. HDT-A is related to the glass transition, while HDT-B is associated with the early stages of the crystal melting process. Indeed, in an unfilled semi-crystalline system it is usual that the two temperatures are different; once the material has passed through the high HDT modulus threshold (Tg), the crystalline structure prevents it from falling to

the second one. This second threshold is not reached until the material approaches the melting point. On the other hand, in an amorphous system no appreciable difference in the two threshold temperatures is usually observed.

3. Results and Discussion

3.1 PLA-silica bio-composite characterization

3.1.1 Morphological analysis

The morphology of the prepared bio-composites was investigated by scanning electron microscopy (SEM). **Figures 2a** and **2b** show two magnifications of PA6.10_20S and **Figures 2c** and **2d** of PA10.10_20S, as examples. Observation with naked eye reveal that composites with 20 wt.% RHA exhibit a homogeneous distribution and a fine dispersion within the polymer matrix, notwithstanding the presence of micrometric particles (50–0.5 μm distribution). Despite this, there is no segregation of the filler; rather there is good adhesion between filler and PLA (**Figures 2b** and **2d**). To evaluate the dispersion and distribution, the two methods described in section 2.4 have been used. As far as the dispersion is concerned, the average percentage deviation from the mean value of particles for each area is assumed as 11, 10, and 12% for PA6.10_10S, PA6.10_20S, and PA6.10_10S5C, respectively. This implies that in every composite with the PA6.10 matrix the dispersion is similar. Indeed, around 10% of difference of particle numbers from one area to another has been found for all formulations.
In the PA10.10-based composites only PA10.10_20S showed a lower deviation (5%) with respect the other that are around 10-12%.

Generally, all the differences are small and have to be mitigated by considering the unavoidable measurement errors. Therefore, could be concluded that there are no great differences in the dispersion of the particles in all studied composites.

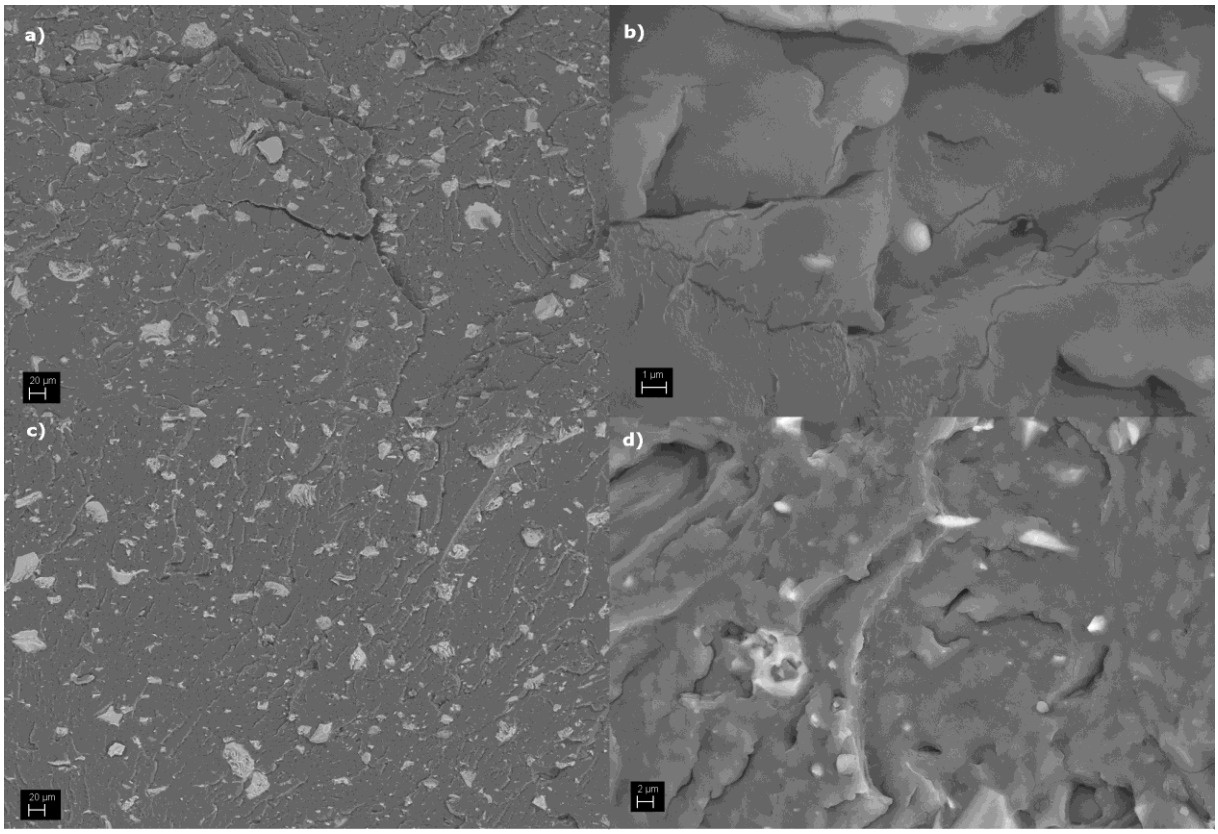


Figure 2. FE-SEM micrographs of: a), b) PA6.10_20S and c), d) PA10.10_20S.

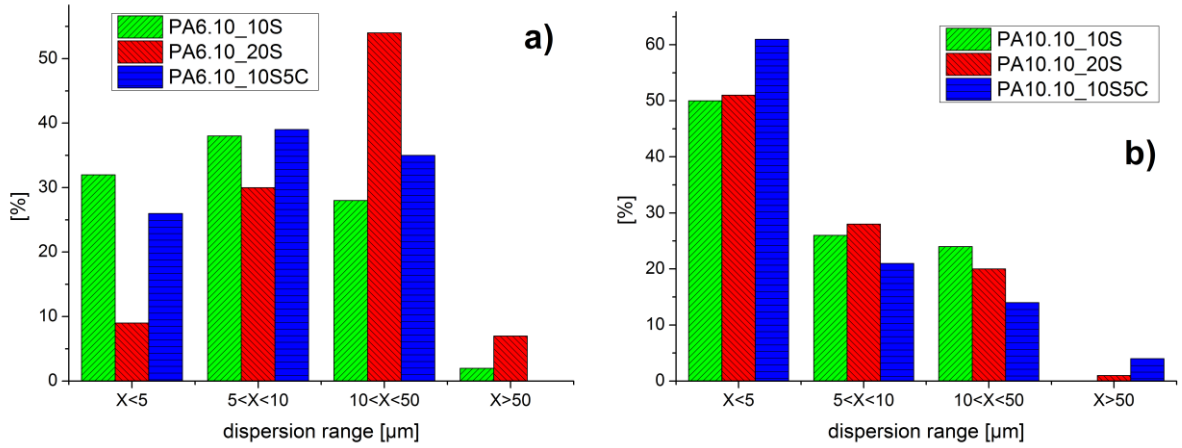


Figure 3. Distribution analysis of: a) PA6.10 and b) PA10.10 composites.

The second parameter taken into consideration for the morphological analysis is the distribution. In this case, the particles have been numbered according to their size. Four ranges have been used from less than 5 μm to more than 50 μm (**Figures 3a** and **b**). The particle distribution in PA6.10_10S and PA6.10_10S5C shows an equal percentage of particles under 50 μm centered in the 5–10 μm region. When a large amount of RHA is added to the composite, the distribution conspicuously moved to bigger particle size with the highest frequency in the 10–50 μm class. Considering PA10.10, the distribution remains quite the same for the two compositions with only RHA, while there is a little increase in the smaller size particles in the case of PA10.10_10S5C. In every case, the most populated range for PA10.10 is the smallest one (under 5 μm). Is it important to remark that in this study, particles under 2–3 μm were not clearly visible in the micrograph, and thus, appropriately counted.

3.1.3 Mechanical properties

The mechanical properties of the prepared bio-composites was thoroughly investigated; to this aim, two different techniques (namely, stress-strain and dynamic thermo-mechanical analyses) have been employed. In long-term use and packaging field, the mechanical and thermo-mechanical properties play a key role in correctly choosing the most suitable material/formulation for obtaining the desired performance.
With this goal, stress/strain analyses at room temperature were performed for assessing the rigidity and toughness of the composites. The collected data are listed in **Table 2** and an exemplificative curve is reported in **Figure 4**. As expected, when a ceramic filler

is added to a polymer matrix, a significant increase of the Young's modulus and decrease in the deformation at break of the two PAs as a function of the RHA content has been observed. The tests have also shown that the addition of RHA, however, caused a decrease in the maximum tensile strength (σ_{max} **Table 2** and **Figure 4**) when compared to the neat matrices. This result is generally caused by the low efficiency of transferring stresses from the matrix to the reinforcement. More specifically, the addition of 20 wt.% of RHA in PA10.10 induces a significant decrease of the σ_{max} and this fact might be explained with the presence of interface defects. To better understand the quality of the interfacial bonding, Pukanszky's model was applied to the different composites using the tensile strength at yield point (σ_y **Table 2** and **Figure 4**). Pukanszky's equation was applied to determine if there is some different interaction between fillers and matrices. As a result of this model, the plot of reduced stress at yield ($\log \sigma_{red}$) as a function of volumetric fractions gives, theoretically, a straight line whose slope represents B. As already explained, B is a term corresponding to the load carrying capability of the filler and depends on the filler-matrix interactions and is influenced by all factors affecting the load-bearing capacity of the filler. One of these factors is the strength of interaction (which depends on surface energy/chemistry of the constituent) and another one is the size of the contact surface [27]. This last aspect has been discussed below.

Figure 5 reports the data of reduced stress at yield as a function of the volumetric fraction. The data obtained from the composites containing only RHA are plotted as the empty marker and the data of composites with both RHA and Cl30B are the fully colored marker. In addition to the plot, an interpolation line between the composites with 10 and 20 wt.% RHA was calculated and shown as the dotted curve.

Comparing the two PA matrices, it is noteworthy that at 10 wt.% loading, the PA10.10 exhibits a higher log σ_{red} value than PA6.10. This trend was also followed by the increase of the E modulus reported in **Table 2** (+35 vs +15%, respectively). If we consider only this point, the B value, and thus, the interactions of the filler-matrix of PA10.10 are almost higher than PA6.10. On the contrary, when we consider the data at 20 wt.%, the tendency is reversed. In-depth analysis shows that at 20 wt.% both matrices exhibit data that is significantly lower than that expected by a linear trend from the first point, but, in the case of PA10.10, this decrease is more noticeable. Such a general trend is usually reported when the filler amount is high and the particles start to interact with each other losing part of their load carrying capability. This behavior does not seem to be correlated with the distribution of particle sizes found. Indeed, in the morphological study, the two PAs have different distribution, thus better performances could be expected from the PA10.10 matrix because smaller particles usually carry bigger loads. On the other hand, interacting stress fields because of particles that are close leads to decreasing stress transfer, and this second aspect seems to be prevalent in the high loading composites. In any case, PA6.10 matrix shows a better interaction with RHA at high filler loading than PA10.10.

In both cases, the calculated interpolation lines are not very close to the two experimental points and are relatively similar. B values of 3.15 and 3.40 have been found for PA10.10 and PA6.10, respectively. From this we can conclude that with both PAs the Pukanszky's interpolation model does not follow the composite behavior closely at high filler content but better confidence values are obtained with PA6.10.

Moreover, the modulus increase is not affected by the different filler distribution of particles, and the two composites, notwithstanding matrix origin, show similar results (+45% with respect to the reference matrix).

Surprisingly, the presence of Cl30B, slightly enhances the strain values of PAs with 10 wt.% RHA. In fact, the distribution of particles, already discussed in section 3.2.1 never showed big differences except for a little increase in the percentage of smaller particles in the PA10.10 matrix. Probably the aspect ratio of the Cl30B lamellae and a partially sub-micrometric exfoliation of montmorillonite generated this increase. The higher filler-matrix interaction level was verified by application of Pukanszky's model: the PA6.10_10S5C and PA10.10_10S5C values represented in **Figure 5** were over the interpolation lines of the corresponding RHA composites. Thus, the derived B values were higher than the corresponding RHA composites (4.94 and 4.80 for PA6.10_10S5C and PA10.10_10S5C, respectively). Finally, the modulus increase data (ΔE in **Table 2**) confirmed better filler-matrix interactions (+94 and +85% with respect to neat matrices for PA6.10 and PA10.10, respectively).

In another study Feldmann et al. [10] studied the mechanical performances of the same two PA filled with man-made cellulose fibers. In this case they reached similar values of modulus with the 15 wt.% load but, conversely to our results, also a significant increase of the tensile strength. This finding is probably due to the better ability of the fibers with respect the particles to transfer stresses. However, the results obtained with the use of RHA are in any case relevant because wastes, that can produce environmental pollution, are used as filler.

To compare our data with another biodegradable matrix, PLA was also investigated. In this case, a B value of 1.47 was found. This data is much lower than that determined for

the PAs, thus, the two PAs have better interactions with RHA than PLA. Regarding the modulus, E, the tests reveal an increase that is only a little lower than that observed with the PA matrices (+40%). In addition, also in the case of the PLA matrix, the presence of Cl30B gave better results for interactions and modulus.

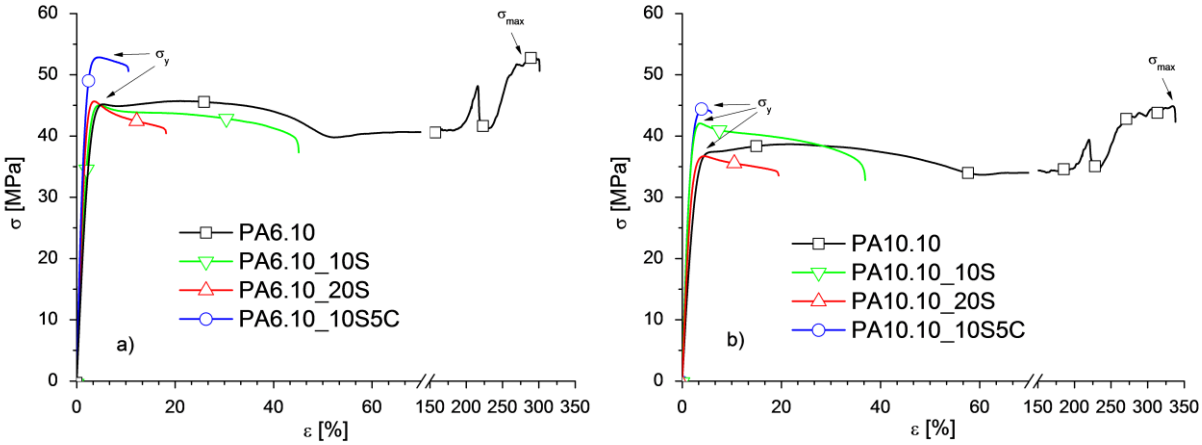


Figure 4. Stress-strain data of a) PA6.10-, b) PA10.10-based composites.

Table 2. Stress-strain and HDT from DMTA data of PA6.10-, PA10.10-, and PLA-based composites.

		PA6.10	10S	20S	10S5C	PA10.10	10S	20S	10S5C	PLA	20S	10S5C
Stress-strain analysis at 23°C	E [GPa]	1.74±0.07	2.00±0.06	2.53±0.15	3.37±0.24	1.45±0.04	1.96±0.04	2.09±0.1	2.68±0.07	3.61±0.12	5.04±0.39	5.53±0.34
	ΔE [%]*	-	+15	+45	+94	-	+35	+44	+85	-	+40	+53
	ε [%]	316±30	44±3	17±3	11±1	343±25	38±5	18±4	5±1.3	3.2±0.6	2.5±0.7	4.8±1.3
	σ_{max} [MPa]	52.7±1.1	45.6±0.4	45.4±0.6	52.1±0.7	46.2±2.0	41.2±0.5	36.4±0.4	44.0±1.7	65.4±1.0	50.1±1.8	57.1±0.7
	σ_y [MPa]	44.8±0.8	45.6±0.4	45.4±0.6	52.1±0.7	38.3±0.3	41.2±0.5	36.4±0.5	44.0±1.7	65.4±1.0	50.1±1.8	57.1±0.7
HDT from DMTA	0.46 MPa [°C]**	138	171	>180	>180	109	144	174	>180	66	68	67
	1.81 MPa [°C]**	59	66	72	91	60	56	61	72	63	64	65

* Δ = E' matrix-E' composite/E' matrix ** Calculated with E' data

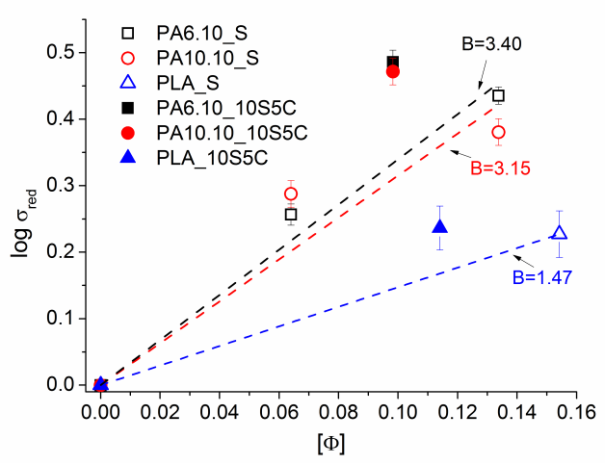


Figure 5. Reduced stress data of PA6.10-, PA10.10-, and PLA-based composites with fitting lines according to Pukanszky's model.

Dynamic thermo-mechanical analysis in the dual cantilever mode was used in order to establish the effect of the temperature and filler content on the storage modulus of bio-PA and PLA. **Figure 6** reports the trend of the storage modulus (E') *vs*. temperature for the PA6.10 (**a**), PA10.10 (**b**), and PLA (**c**). As already discussed, the thermo-mechanical aspect is fundamental for those applications at conditions different from room temperature. Moreover, one of the main drawbacks of several renewable polymers is their poor mechanical properties with increasing temperature. Indeed the two PAs and PLA show similar HDT-A at around 60°C. For all the formulations with PLA, the mechanical property collapse occurs around 65°C. DMTA data confirm that PLA and also the bio-composites, regardless of their filler content and type, may be used only below 60–65°C, where the mechanical properties decrease dramatically. This behavior is industrially referenced by a single data point called HDT, as mentioned previously. PLA is mostly an amorphous system; thus, the two loads of HDT are not appreciably different, as reported in **Table 2** (66 and 63°C). Conversely, if we examine the HDT tabular data for unfilled PAs, we find a great difference between the values

measured at 0.455 MPa and 1.82 MPa because of the semi-crystalline composition. PA10.10 shows a difference of 50°C from HDT-A to B, while PA6.10 shows as much as 80°C.

Once the composites with RHA were tested, from an overall consideration, a general increase in E' was observed for all the prepared composites, as expected from the stress-strain analyses. In addition, E' turned out to be a function of the RHA content: it increases with increasing filler content. Moreover, at high temperatures (>100°C), the bio-composites exhibited higher storage modulus than that of their corresponding matrices (**Figure 6**). Thus, the HDT-A increases simply because the material is now rigid enough to remain above the 800 MPa threshold. This increase is evident with PA6.10 (+13°C), while quite negligible with PA10.10 or PLA (+1°C). The behavior became significant if HDT-B is considered. Indeed, in this case, the enhancements were >40 and 65°C for PA6.10 and PA 10.10, respectively, while PLA does not show any significant effect. In fact, because of the amorphous nature of PLA, there are no differences between HDT-A and HDT-B.

The best stress-strain and filler-matrix interaction performances found with Cl30B addition were also reflected in the HDT values. In particular, HDT-A is highly affected: PA6.10 and PA10.10 show an increase of 32°C and 12°C. For HDT-B, both PAs reveal a temperature resistance over 180°C, which was the end of the test. Additionally, in this case, no relevant changes were registered with PLA.

Also in this case the bioPAs prepared with cellulose [10] showed better results increasing the HDT over 160°C.

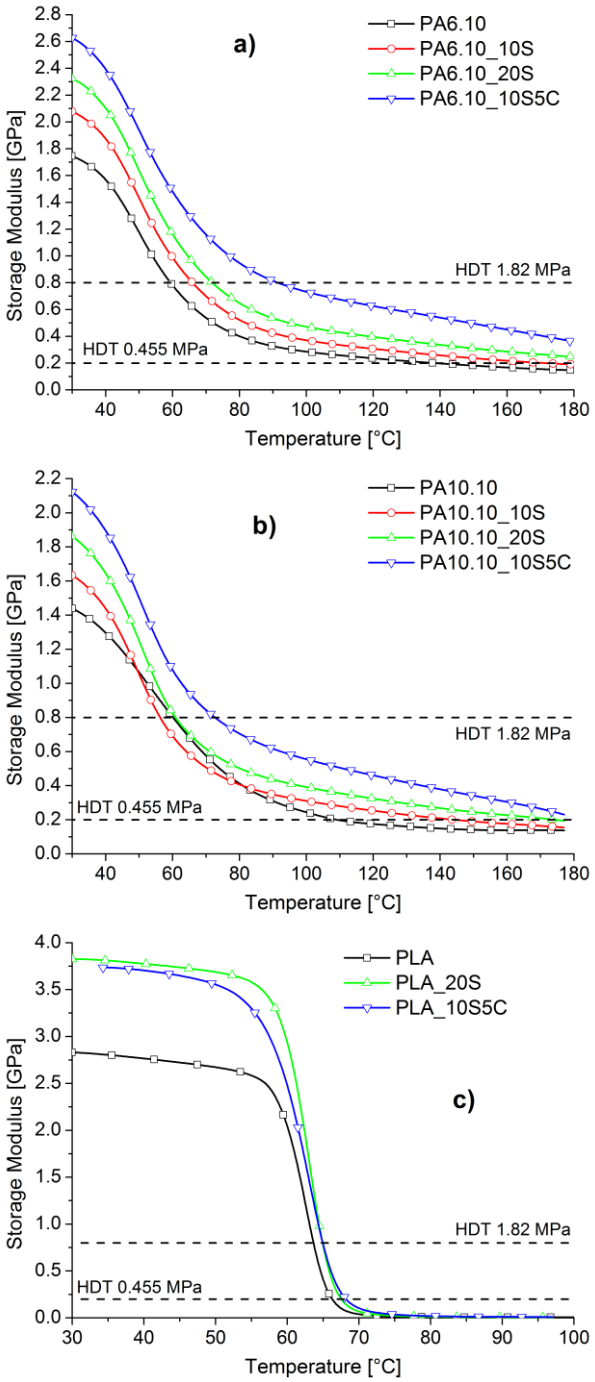


Figure 6. Storage modulus E' of a) PA6.10-, b) PA10.10-, and c) PLA-based composites with 1.82 and 0.455 MPa HDT lines.

4. Conclusions

In this study, composites consisting of fully renewable polyamide PA10.10, partially renewable PA6.10 and poly(lactic acid) were melt compounded with a renewable by-product,

rice husk ash (RHA). The possibility of obtaining injection-molded specimens was verified by preparing samples for the mechanical analyses. The data collected from the stress-strain analyses showed that RHA induced significant improvement in the Young's modulus, as well as a slight reduction in the tensile strength, and a large decrease in the deformation at break, as a function of the RHA content.

The application of the Pukanszky's model do not closely follow the composite behavior from 10 to 20 wt.% loading. At the high filler loading there is a loss of matrix-filler interactions, which is more evident with the PA10.10. The ability of RHA to reinforce the two PAs is similar and better with respect to PLA. The morphology studies demonstrate that interactions at high filler content are mainly dominated by other factors than the distribution of particles sizes.

A second important achievement was obtained with the addition of modified clay to the used PA-systems. In this case, the best mechanical properties and filler-matrix interactions were observed, notwithstanding the matrix used.

Finally, DMT analyses have also shown that the addition of RHA caused an increase in the HDT when compared to the PA matrices alone. Furthermore, the simultaneous presence of RHA and clay gave the best results. The achieved HDT-A (1.82 MPa) temperatures turned out to higher the field of applications of the two PAs, especially for PA6.10, which achieved an increase of 32°C. Moreover, the PAs do not show a drastic decrease in the properties after the first HDT, like PLA. This behavior allows HDT-B (0.455 MPa) values to rise to more than 180°C with the use of 10 wt.% RHA and 5 wt.% Cl30B.

Acknowledgements

The Authors would like to thank Mr. Simone Infantino for the compounding of the materials.

ABBREVIATIONS

RHA, rice husk ash; PA, polyamide; PLA polylactic acid; HDT, heat deflection temperature; DMTA, dynamic mechanical thermal analysis; RH, rice husk; Cl30B, Cloisite®30B; SEM, Scanning Electron Microscope; HMDA, hexamethylene diamine; Tg, .glass transition temperature.

References

[1] http://en.european-bioplastics.org/market/

[2] Ruehle D A., Perbix C, Castañeda M, Dorgan JR, Mittal V, Halley P, et al. Blends of biorenewable polyamide-11 and polyamide-6,10. Polymer 2013;54:6961–70. doi:10.1016/j.polymer.2013.10.013.

[3] Xiuwei F, Xiaohong L, Laigui Y, Zhijun Z. Effect of in situ surface-modified nano-SiO 2 on the thermal and mechanical properties and crystallization behavior of nylon 1010. J Appl Polym Sci 2010;115:3339–47. doi:10.1002/app.30457.

[4] Battegazzore D, Alongi J, Fontaine G, Frache A, Bourbigot S, Malucelli G. Bulk vs. surface flame retardancy of fully bio-based polyamide 10,10. RSC Adv 2015;5:39424–32. doi:10.1039/C5RA04149J.

[5] Taj S, Munawar M, Khan S. Natural fiber-reinforced polymer composites. Proceedings-Pakistan Acad 2007;44:129–44.

[6] Mohanty AK, Misra M, Hinrichsen G. Biofibres, biodegradable polymers and biocomposites: An overview. Macromol Mater Eng 2000;276-277:1–24. doi:10.1002/(SICI)1439-2054(20000301)276:1<1::AID-MAME1>3.0.CO;2-W.

[7] Battegazzore D, Bocchini S, Alongi J, Frache A, Marino F. Cellulose extracted from rice husk as filler for poly(lactic acid): preparation and characterization. Cellulose 2014;21:1813–21. doi:10.1007/s10570-014-0207-5.

[8] Battegazzore D, Bocchini S, Alongi J, Frache A. Rice husk as bio-source of silica: preparation and characterization of PLA-silica bio-composites. RSC Adv 2014;4:54703–12. doi:10.1039/C4RA05991C.

[9] Feldmann M et al. Influence of the process parameters on the mechanical properties of engineering biocomposites usinga twin-screw extruder. Composites: Part A (2015), http://dx.doi.org/10.1016/j.compositesa.2015.03.028.

[10] Feldmann M, Bledzki AK. Bio-based polyamides reinforced with cellulosic fibres – Processing and properties. Compos Sci Technol 2014;100:113–20. doi:10.1016/j.compscitech.2014.06.008.

[11] FAO Rice Market Monitor, July 2015, Vol. XVIII, www.fao.org/economic/RMM

[12] Prasad R, Pandey M. Rice Husk Ash as a Renewable Source for the Production of Value Added Silica Gel and its Application: An Overview. Bull Chem React Eng Catal 2012;7. doi:10.9767/bcrec.7.1.1216.1-25.

[13] Soltani N, Bahrami A, Pech-Canul MI, González LA. Review on the physicochemical treatments of rice husk for production of advanced materials. Chem Eng J 2014;264:899–935. doi:10.1016/j.cej.2014.11.056.

[14] Tsai WT, Lee MK, Chang YM. Fast pyrolysis of rice husk: Product yields and compositions. Bioresour Technol 2007;98:22–8. doi:10.1016/j.biortech.2005.12.005.

[15] Patel M, Karera A, Prasanna P. Effect of thermal and chemical treatments on carbon and silica contents in rice husk. J Mater Sci 1987;22:2457–64. doi:10.1007/BF01082130.

[16] Turmanova S, Genieva S, Vlaev L. Obtaining Some Polymer Composites Filled with Rice Husks Ash-A Review. Int J Chem 2012;4:62–89. doi:10.5539/ijc.v4n4p62.

[17] Chaudhary DS, Jollands MC, Cser F. Recycling rice hull ash: A filler material for polymeric composites? Adv Polym Technol 2004;23:147–55. doi:10.1002/adv.20000.

[18] Ayswarya EP, Vidya Francis KF, Renju VS, Thachil ET. Rice husk ash – A valuable reinforcement for high density polyethylene. Mater Des 2012;41:1–7. doi:10.1016/j.matdes.2012.04.035.

[19] Arayapranee W, Naranong N, Rempel GL. Application of rice husk ash as fillers in the natural rubber industry. J Appl Polym Sci 2005;98:34–41. doi:10.1002/app.21004.

[20] Siriwardena S, Ismail H, Ishiaku US. A Comparison of the Mechanical Properties and Water Absorption Behavior of White Rice Husk Ash and Silica Filled Polypropylene Composites. J Reinf Plast Compos 2003;22:1645–66. doi:10.1177/073168403027619.

[21] Fuad MYA, Ismail Z, Mansor MS, Ishak ZAM, Omar AKM. Mechanical Properties of Rice Husk Ash/Polypropylene Composites. Polym J 1995;27:1002–15. doi:10.1295/polymj.27.1002.

[22] Kojima Y, Usuki A, Kawasumi M, Okada A, Kurauchi T, Kamigaito O. Synthesis of nylon 6–clay hybrid by montmorillonite intercalated with ϵ-caprolactam J Polym Sci Part A: Polym Chem 1993;31:983-6. doi:10.1002/pola.1993.080310418.

[23] Liu Z, Zhou P, Yan D. Preparation and properties of nylon-1010/montmorillonite nanocomposites by melt intercalation. J Appl Polym Sci 2004;91:1834–41. doi:10.1002/app.13336.

[24] US PATENT 2696500

[25] FR PATENT 1160486

[26] Pukánszky B. Influence of interface interaction on the ultimate tensile properties of polymer composites. Composites 1990;21:255–262. doi: 10.1016/0010-4361(90)90240-W

[27] Dorigato A, Sebastiani M, Pegoretti A, Fambri L. Effect of Silica Nanoparticles on the Mechanical Performances of Poly(Lactic Acid). J Polym Environ 2012;20:713–25. doi:10.1007/s10924-012-0425-6.

[28] Lazzeri A, Phuong VT. Dependence of the Pukánszky's interaction parameter B on the interface shear strength (IFSS) of nanofiller- and short fiber-reinforced polymer composites. Compos Sci Technol 2014;93:106–13. doi:10.1016/j.compscitech.2014.01.002.

[29] Takemori MT. Towards an understanding of the heat distortion temperature of thermoplastics. Polym Eng Sci 1979;19:1104–1109. doi: 10.1002/pen.760191507